Observations of on-demand quantum correlation using Poisson-distributed photon pairs

by S. Kim and B. S. Ham
GIST, S. Korea

A. Poisson statistics

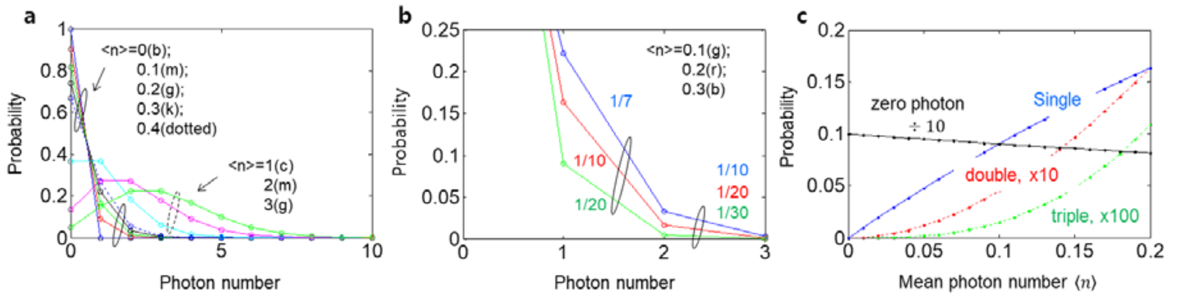

Fig. S1. Numerical calculations of Poisson distribution. (a) Probability vs. photon number. (b) Probability vs. photon number (expanded of a), where the number indicates a ratio η, $\eta = p(N+1)/p(N)$. (c) Probability vs. mean photon number.

In the theory of individual photon statistics, the Poisson distribution (probability) is described as follows:

$$p(n, N) = \frac{n^M e^{-n}}{M!}, \qquad \text{(S1)}$$

where n is mean photon number, and M is the number of occurrence (observation). Using equation (S1), numerical calculations with respect to mean photon number and photon number occurrence are calculated in Fig. S1. In Fig. S1b, relative occurrence ratios calculated for the mean photon number in Fig. S1(a). According to the numerical calculations, the ratio of doubly bunched photon to single photon is 1/7, 1/10, and 1/20 for the mean photon number of $\langle n\rangle = 0.3, 0.2,$ and 0.1, respectively (see Figs. S1(b) and (c)). The best fit curve for these ratios roughly follows $c/\langle n\rangle$, where c is an adjust constant. The higher order ratio rapidly decreases. As an example, for $\langle n\rangle = 0.1$, the doubly bunched photon occurrence to the single photon one is 0.5%, while the triple photon occurrence to the single (double) photon is 1/600 (1/30).

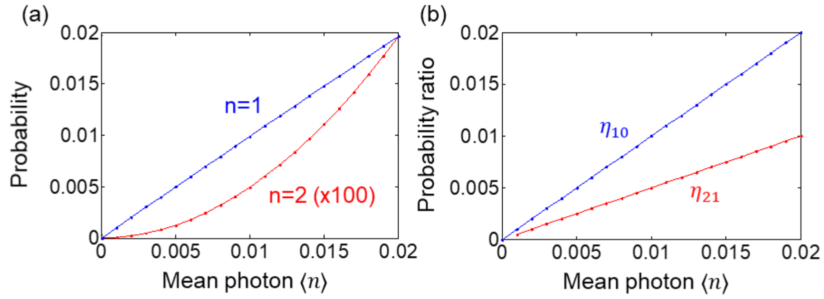

Fig. S2. Numerical calculations for Poisson distribution. $\eta_{ij} = \frac{P(n=i)}{P(n=j)}$. (a) Photon probability vs. mean photon number. (b) Photon probability ratio.

Using equation (S1), Poisson distribution is calculated in Fig. S2 for n=1 and n=2 with respect to mean photon number $\langle n\rangle$. For $\langle n\rangle = 0.01$, double to single photon generation rate is $\eta_{21} = 0.005$ (see the red line). Thus, the higher order (n>2) bunched photon generation except for the doubly bunched photon (n=2) is neglected.

B. An asymmetric PZT scan method to induce decoherence

The coherent light source of HeNe laser has a typical coherence length of 30 cm, whose corresponding bandwidth is 1 GHz. This bandwidth is due to the inhomogeneity of HeNe laser by Doppler broadening, where individual photon's linewidth is about 1 kHz determined by the decay process from $3S_2$ to $2P_4$ of Ne atoms at $\lambda = 632.8$ nm. In other words, the coherence length of each single photon is comparable to 300 m. Thus, the coincidence detection in the scan range of a few microns has no practical meaning as in most HOM dip experiments.

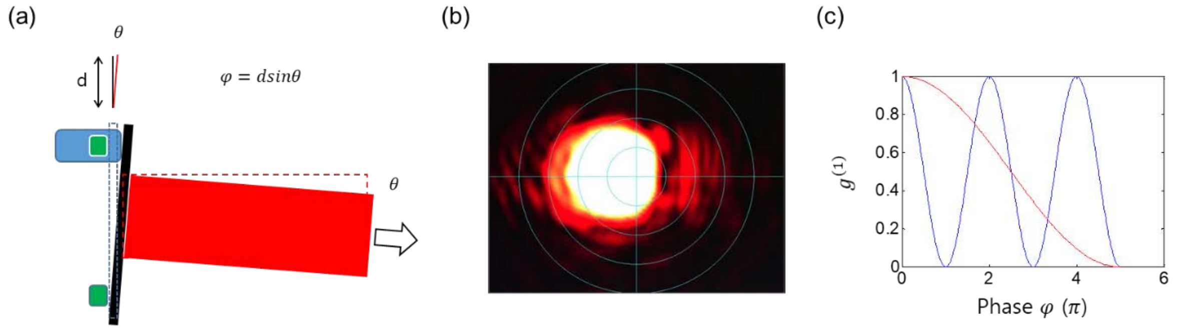

Fig. S3. Asymmetric PZT scanning to induce decoherence. (a) Side view of PZT actuator. (b) A PZT controlled beam walk-off. (c) Numerical simulation for (a) and (b).

For the intentional decoherence induction in measurements, a PZT scanning method is set to be asymmetric with respect to the wave front on the second BS of MZI. For the asymmetric PZT scanning, only one axis of a three-axis PZT actuator is scanned, resulting in linear phase increase in the cross section as shown in Figs. S3(a) and S3 (b). Because whole interacting light is captured by SPCM, the number of interference fringe to be detected increases as the scanning length increases. For the symmetric phase control effect, the position walk-off induces position-dependent phase increase, $\varphi = \mathrm{d}\sin\theta$, where d is the beam diameter and θ is the PZT scan dependent angle from the horizon. Because the single photon detector captures the whole area of the beam cross section, the walk-off induced phase incoherence increases, resulting in coherence washout as shown in Fig. S3(c). This is the origin of intentional decoherence in the present experimental scheme for Fig. 1.

Figure S3(c) is numerical simulations for the asymmetric PZT scanning. For simplicity, the position of cross section is set to be one dimensional, and the scanning is replaced by a relative phase φ, in which the same proportional constant is multiplied to both variables. Then, the resulting interference fringe is averaged for the final measurement corresponding to the signal. The blue curve is the reference without walk-off, while the red curve is for the walk-off. This effect is the same as the typical phenomenon observed with wide bandwidth light source. When the modulation visibility reaches zero, it resembles incoherence particles. For the classical bound with individual and incoherent photons, $g^{(2)}(0) = 0.5$. For coherent photons, $g^{(2)}(0) = 1$. Thus, we can set the reference values for the intensity correlation of $g^{(2)}(\tau)$ for these known cases. Here, the higher order bunched photon effects are neglected as discussed in Section A (see Fig. S1).

C. Measurements of Poisson distributed photon statistics using a coincidence counting module (CCM)

Table S1. Photon statistics from the attenuated He/Ne laser. N_A: single photon detection counting number in path A, N_B: single photon detection counting number in path B. N_{AB}: coincidence detection counting number between path A and B. $\eta_{21} = \frac{N_{AB}}{N_A+N_B}$: doubly-photon to single-photon counting ratio.

single count rate	single count rate	coincidence count rate	(C*2/(A+B))*100
count/s	count/s	count/s	%
D1	D2	D1&D2	coincidence vs single
108.55	108.71667	0	0
208.46667	206.05	0	0
309.61667	311.78333	0	0
422.66667	416.48333	0	0
501.51667	496.53333	0	0
614.15	594.56667	0	0
693.95	688.75	0	0
859.81667	829.48333	0	0
907.15	887.8	0.01667	0.00186
1032.75	1011.21667	0.01667	0.00163
2080.55	2008.26667	0.03333	0.00163
3014.2	2990.4	0.08333	0.00278
3958.25	3899.15	0.2	0.00509
5041.06667	4968.63333	0.33333	0.00666
6038.85	5963.25	0.35	0.00583
7051.18333	6936.96667	0.6	0.00858
8164.2	8074.16667	0.93333	0.0115
9192.06667	9072.66667	1.25	0.01369
10119.26667	10007.48333	1.03333	0.01027
20794.15	20554.7	5.45	0.02636
30798.78333	30257.58333	10.78333	0.03532
40380.76667	39791.18333	18.75	0.04677
50836.5	50262.81667	29.48333	0.05833
60130.5	59364.56667	41.43333	0.06935
69842.41667	70171.15	56.8	0.08113
80365.03333	80792.95	74.33333	0.09225
90692.33333	91168.93333	93.28333	0.10259
100541.86667	100969.01667	115.73333	0.11487
204795.2	205945.7	483	0.23518
303525.3	303485.71667	1058.86667	0.34888
403416.1	402076.08333	1856.66667	0.461
501252.43333	500243.03333	2870.13333	0.57317
602435.76667	602038.75	4151.51667	0.68935
700272.25	700171.38333	5615.28333	0.80193
803240.31667	804089.28333	7398	0.92053
901106.16667	904817.15	9328.06667	1.03305
1004965.2	1008626.73333	11565.18333	1.14871
2010027.25	2019053.73333	46219.25	2.29428
3064911.43333	3082731.66667	107370.85	3.49307
3994814.56667	4021282.58333	182517.23333	4.55377
5035333.8	5068910.81667	289603.21667	5.73231
5982037.6	6028272.1	408298.36667	6.79913
6930970.55	7088833.11667	511513.9	7.29702
8100109.8	8175300.83333	686903.53333	8.441
9022735.26667	9035251.13333	843985.63333	9.34751
1.0043E7	1.03505E7	1072772.76667	10.52073

Table S1 shows the measurement results by CCM. The first two columns (N_A and N_B) are for single photon detection counting numbers from MZI paths B and A without BS2 in Fig. 1, respectively, for different ODs of ND filters. The third column (N_{AB}) is for the coincidence detection measurements between A and B with BS2. The last column is the corresponding ratio of the coincidence detection (N_{AB}) to single photon counting ($N_A + N_B$) numbers.

D. Measurements of Poisson distributed photon statistics using a fast oscilloscope

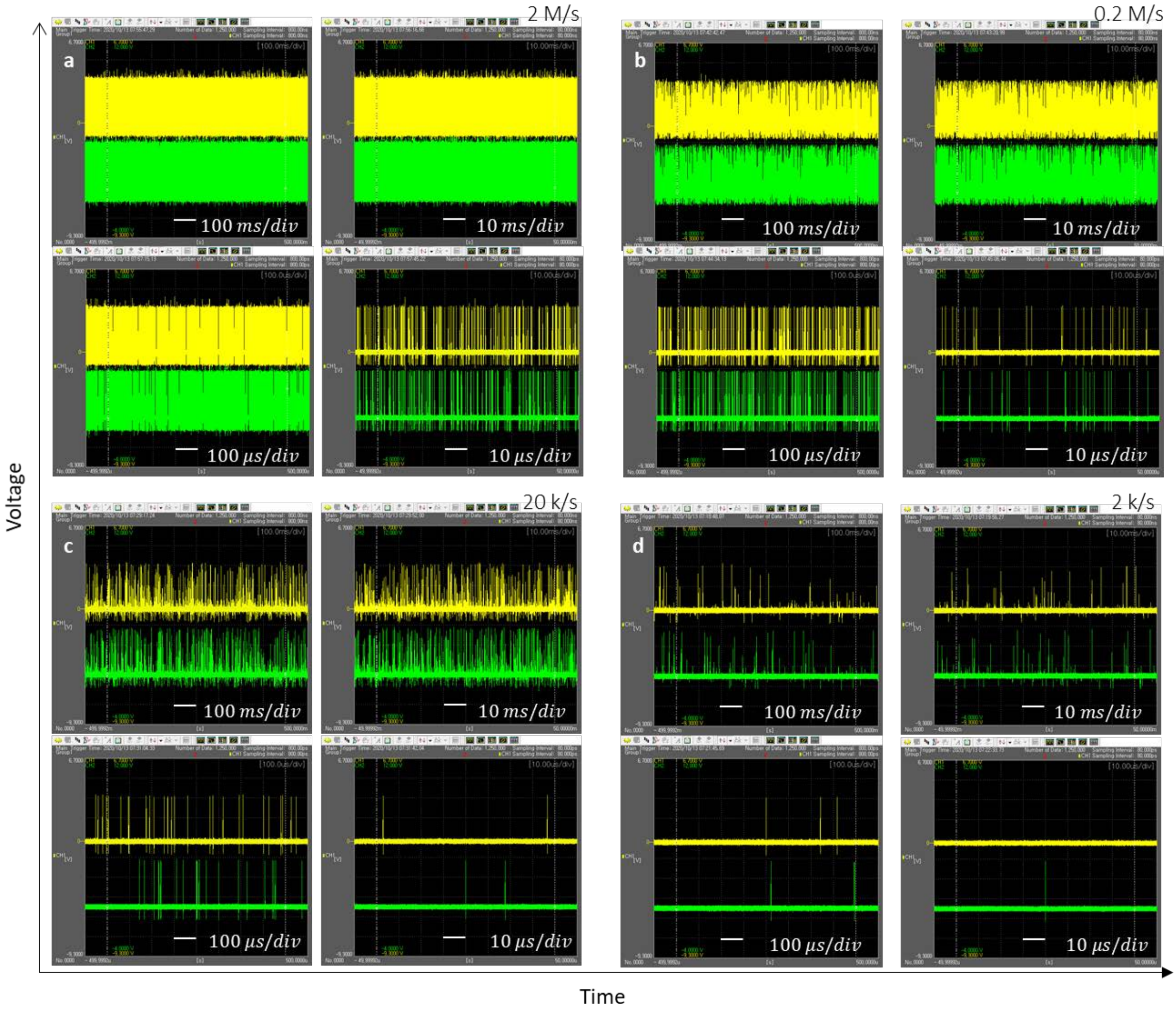

Fig. S4. Poisson distributed photon streams captured on oscilloscope screen. Horizontal: time; Vertical: voltage. Each pulse voltage is set to be 4 V by SPCM module. Yellow and green for the captured in each MZI path.

Figure S4 is the screen captures for the observations of Poisson distributed photon generations by an attenuated typical HeNe laser (JDS Uniphase, Novette 1508-0). The light polarization of HeNe laser is random. For the attenuation, several ND filters (fixed and variable) are combined for different optical densities. There are four different photon counting cases in four different time scales in Fig. S4. Once a single photon is detected by SPCM (Excelitas AQRH-SPCM-15), its output signal is fixed at 4V with 10 ns pulse duration. As the single photon counting rate is separately measured by a coincidence counting module (CCM, Altera DE2), photon characteristics of antibunched and bunched photons are measured. As attenuation increases from Fig. S4(a) to Fig. S4(d), the mean photon number decreases as discussed in Fig. 1. The ratio of doubly bunched photons to single photons is also measured to confirm the CCM-based numbers in Fig. 3 of the main text.